

# MISSING DARK MATTER IN THE LOCAL UNIVERSE

I. D. Karachentsev<sup>1</sup>

<sup>1</sup>*Special Astrophysical Observatory of the Russian AS, Nizhnij Arkhyz 369167, Russia*

A sample of 11 thousand galaxies with radial velocities  $V_{LG} < 3500$  km/s is used to study the features of the local distribution of luminous (stellar) and dark matter within a sphere of radius of around 50 Mpc around us. The average density of matter in this volume,  $\Omega_{m,loc} = 0.08 \pm 0.02$ , turns out to be much lower than the global cosmic density  $\Omega_{m,glob} = 0.28 \pm 0.03$ . We discuss three possible explanations of this paradox: 1) galaxy groups and clusters are surrounded by extended dark halos, the major part of the mass of which is located outside their virial radii; 2) the considered local volume of the Universe is not representative, being situated inside a giant void; and 3) the bulk of matter in the Universe is not related to clusters and groups, but is rather distributed between them in the form of massive dark clumps. Some arguments in favor of the latter assumption are presented. Besides the two well-known inconsistencies of modern cosmological models with the observational data: the problem of missing satellites of normal galaxies and the problem of missing baryons, there arises another one—the issue of missing dark matter.

## 1. INTRODUCTION

Different cosmological models are commonly tested based on the observations of distant objects with redshifts of  $z = v/c \sim 1$  and properties of the cosmic background radiation generated at the epoch of  $z \sim 10000$ . However, the structure and kinematics of nearby ( $z \simeq 0$ ) volumes of the Universe is also an important source of cosmological data. In the Local universe, conditionally limited within the radius of  $D = 10$  Mpc, a large number of dwarf galaxies was found, the velocities and distances of which are tracing the Hubble flow with an unprecedented detail, as compared with distant objects. The studies of stellar population of nearby galaxies allow to recover the history of star formation in them with a resolution of  $\Delta T \sim 10^8\text{--}10^9$  yr. In fact, over the past 10–15 years the study of the Local universe has become an independent and fruitful branch of observational cosmology, which has been repeatedly emphasized by Peebles [1–3].

Until recently, the scarcity of data on the distances of even the closest galaxies was the major obstacle in the development of observational cosmology in the Local universe. Deployment of unique capabilities of the Hubble Space Telescope, combined with a new method for determining the distances to galaxies by the luminosity of the tip of the red giant branch (TRGB) [4] allowed to carry out mass distance measurements of more than 250 nearby galaxies with an accuracy of 5–10%.

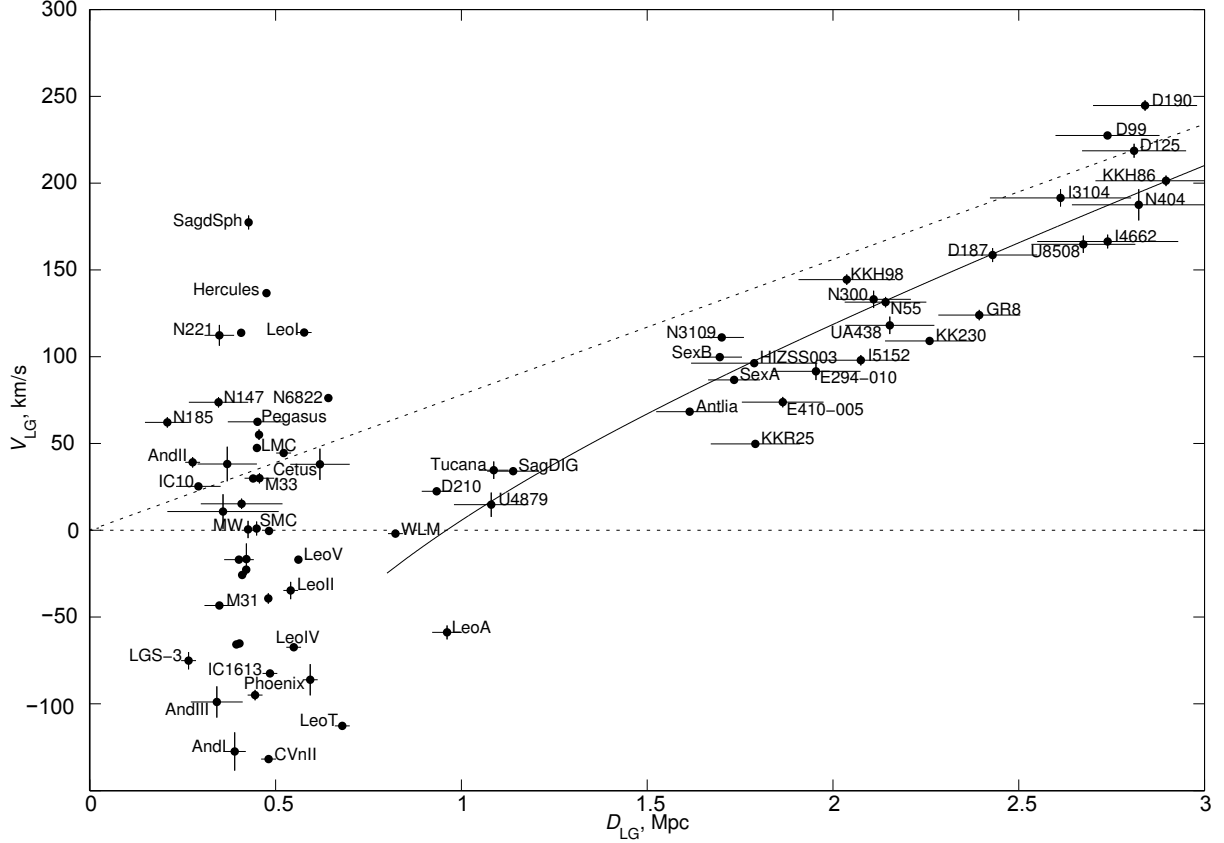


**Figure 1.** The Hubble diagram for galaxies in the vicinity of the Local Group. The distances and velocities of galaxies are given with respect to the centroid of the Local Group, supplemented with error bars. The dashed line corresponds to the undistorted Hubble flow with the parameter  $H_0 = 80$  km/s/Mpc. The curved solid line describes the dragging effect on the flow by the Local Group with a mass of  $1.9 \times 10^{12} M_\odot$ .

The summary of data on distances, radial velocities and other parameters of galaxies in the Local Volume within a radius of 10 Mpc was presented in the Catalog of Neighboring Galaxies (CNG, [5]), which contains 450 objects. In this volume, where the dwarf galaxies down to the luminosities of 10 000 times lower than that of the Milky Way are visible, there are more than a dozen groups, similar to our Local Group in size and population. A detailed pattern of motions of galaxies in these groups and around them has for the first time revealed unexpected features in the Hubble flow at small (1–3 Mpc) scales. It turned out that the Hubble velocity–distance diagrams around the Local Group and other neighboring groups are characterized by a small dispersion of peculiar velocities  $V_{\text{pec}} \sim 30$  km/s. With such small chaotic motions and minor distance measurement errors, a distortion of the “cold” Hubble flow becomes noticeable, caused by the gravitational drag of the galaxies, surrounding the group, by the total mass of the group itself.

An example of the Hubble flow around our group is demonstrated in Fig. 1. This diagram exhibits the region of virial motions of  $\pm 200$  km/s in the companions of the Milky Way and M 31 (Andromeda) and the region of the total Hubble expansion. They are separated from each other by the “zero-velocity sphere” with the radius of  $R_0 = (0.96 \pm 0.03)$  Mpc [6]. It is noteworthy that the radius  $R_0$  determines the total mass of the group,  $M_T = (1.9 \pm 0.2) \times 10^{12} M_\odot$ , and this value is in a remarkable agreement with the virial mass estimates of  $M(\text{MW} + \text{M 31}) = (1.6 \div 2.2) \times 10^{12} M_\odot$ . It should be emphasized that the listed value of  $M_T$  is obtained in assumption of the standard  $\Lambda$ CDM cosmological model with the parameter  $\Omega_\lambda = 0.73$ . In the absence of the  $\lambda$  term ( $\Omega_\lambda = 0$ ), the estimate of the total mass via external galaxy motions would only amount to  $1.2 \times 10^{12} M_\odot$ , i.e. lower than the virial estimates. A similar conclusion can be drawn from the motions of galaxies around the neighboring groups, which are dominated by the M 81 and Centaurus A galaxies [7]. Therefore, the observed features of the local Hubble flow give (at the recently achieved distance measurement accuracy) a direct and independent evidence of the presence in the Universe of a specific cosmic component, the dark energy, discovered from the observations of distant Supernovae.

Recent massive sky surveys both in the optical range, and at the radio line wavelength of 21 cm led to the discovery of numerous nearby dwarf galaxies. An updated version of the CNG catalog now consists of about 800 objects and is currently prepared for print [8].

## 2. FROM LOCAL VOLUME, $D < 10$ MPC, TO LOCAL UNIVERSE, $D < 50$ MPC

High density of observational data on the galaxies in the Local Volume allows us to have a fairly complete conception of the spatial distribution of luminous and dark matter in it. However, on the scale of  $D \sim 10$  Mpc relative fluctuations of the luminosity density amount to  $\Delta\rho_L/\overline{\rho_L} \sim 1$ . This is why the Local Volume cannot be considered representative in terms of its kinematics and dynamics. To achieve a better representation of the observational sample, Makarov and Karachentsev [9] have examined a 100 times larger volume of space around our Galaxy. This volume includes all known galaxies with radial velocities  $V_{LG} < 3500$  km/s relative to the centroid of the Local Group after deduction of the zone of strong extinction at Galactic latitudes  $|b| < 15^\circ$ . This volume with a diameter of 96 Mpc (at  $H_0 = 73$  km/s/Mpc) contains about 11 thousand galaxies. Most of them belong to the Local Supercluster, but this volume (called the “Local universe”) embraces the ridges

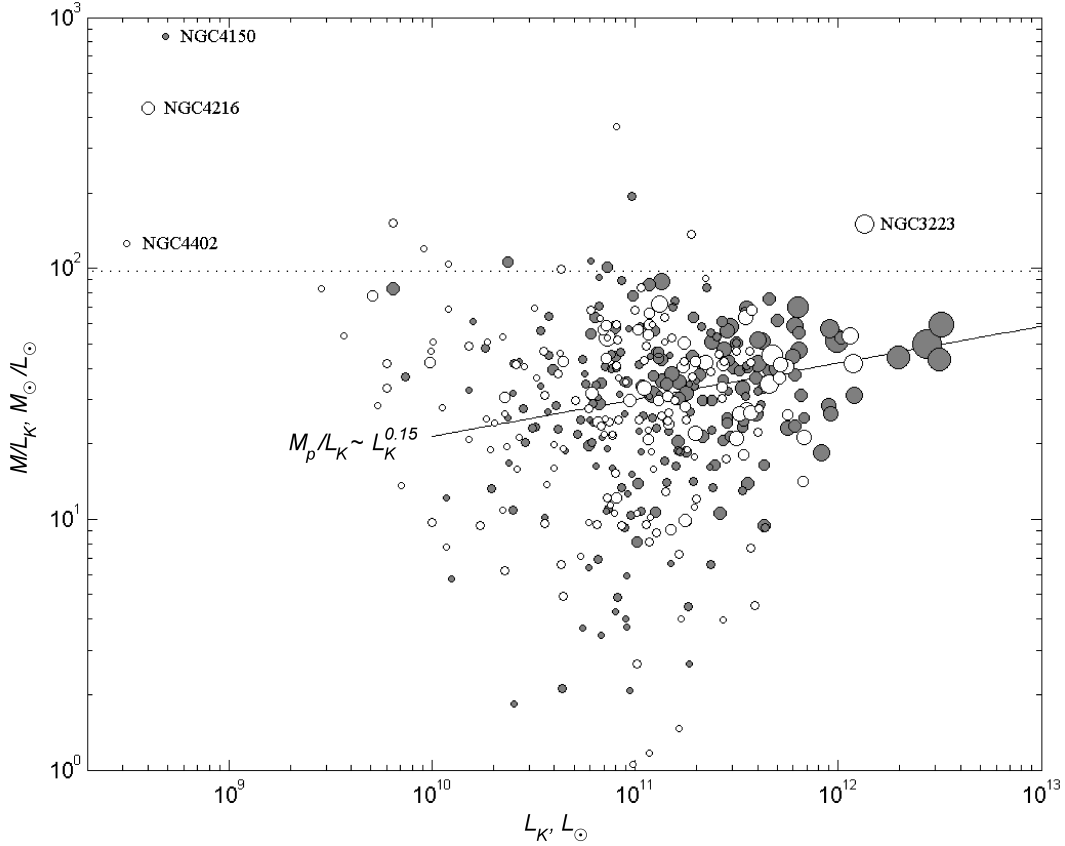


**Figure 2.** The distribution of groups of galaxies with 4 or more members by the integral  $K$ -band luminosity and the virial mass-to-luminosity ratio. The size of the circle depicts the population of the system. Dark circles mark the groups and clusters, where the brightest galaxy has an early morphological type (E, S0, Sa).

of other neighboring superclusters. Based on the data of the Sloan Digital Sky Survey [10], Papai and Szapudi [11] have estimated that the variations of luminosity in galaxies in the cube with an edge of 100 Mpc are about 10%. Consequently, the considered volume of Local universe satisfies quite well the condition of sample representativeness.

The main efforts in our program were aimed at the systematization of data on radial velocities, apparent magnitudes and morphological types of galaxies. At that, we made a search for new dwarf galaxies and performed optical identification of HI radio sources from the HIPASS [12], ALFALFA [13] and other “blind” sky surveys. Particular attention was paid to the problem of the so-called “astro-span”: frequent cases of confusion with the identification of HI sources, the superposition of a star over a galaxy image, when a nearly zero velocity of the star was attributed to a distant galaxy, the cases of a false multiplicity of galaxies, when two or more clumps in it were mistaken for dynamically different objects, etc.

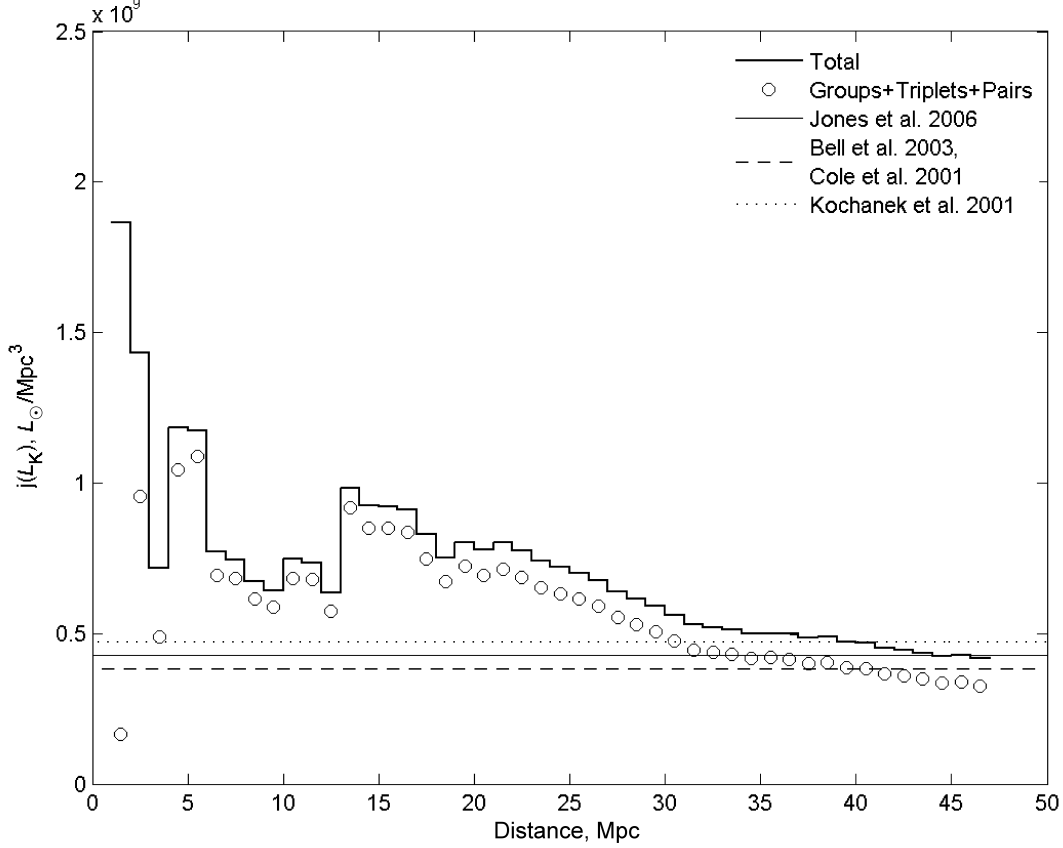


**Figure 3.** The mean density of  $K$ -luminosity of the Local universe in the spheres of different radii (the stepped line). The circles mark the contribution of galaxies in groups, triplets and pairs. The four horizontal lines fix the global value of the luminosity density according to different authors.

Makarov and Karachentsev [9] have applied a new algorithm for identifying the groups with different populations  $n$  to the updated and “cleaned” sample of 10 900 galaxies. In contrast to the simple “friends of friends” (FoF) percolation algorithm [14], the grouping criterion we used took into account the individual luminosities of galaxies. At the primary stage of combining two given galaxies in a virtual pair it was assumed that this pair should have a negative total energy and its components must be causally related (the “crossing time” of a pair is shorter than the age of the Universe). As shown by the subsequent analysis, used in [9], the algorithm isolates groups with approximately the same characteristics both in the nearby, and distant volumes of the Local universe. (Note that the above mentioned FoF criterion does not possess this property). As a result, the following catalogs were compiled: 509 pairs [15], 168 triple systems [16], 395 groups with the population of  $n > 3$  [9] and 520 very isolated galaxies [17].

Not going into detail, note that the pairs, groups and clusters in the Local universe, selected

by this algorithm are in good correspondence with the previously known systems. In some cases, however, the new criterion breaks the known galaxy aggregates into subsystems, which are obviously associated with each other, but have not yet reached the stage of merging and relaxation. Ignoring the substructure of such entities markedly overstates the estimate of their virial mass.

The distribution of groups of galaxies with a population of  $n > 3$  by the integral  $K$ -band luminosity and the virial (projected) mass-to-luminosity ratio is shown in Fig. 2 [9]. The groups, where the main galaxy belongs to the early ( $T < 3$ ) or late types, are represented by shaded and empty circles, respectively, the sizes of the circles are proportional to the group population. The dashed horizontal line in the figure at  $M/L_K = 97 M_\odot/L_\odot$  corresponds to the global average density of matter  $\Omega_m = 0.28$ .

A considerable scatter of galaxy systems in this diagram is primarily due to the projection factors. Despite the large variations, the average virial mass-to-luminosity ratio grows with an increase in the system population or luminosity and is correlated with the morphological type of the brightest member. All these features are well known from other catalogs of groups and clusters of galaxies.

Possessing the data on the luminosities of galaxies in the Local universe, Makarov and Karachentsev [9] have traced the variation of the mean luminosity density in the  $K$ -band depending on the radius of the sphere, within which the averaging is carried out. The dependence of the mean density  $j(L_K)$  on distance  $D$  is presented in Fig. 3 with a step of 1 Mpc. As we can see, the main contribution to the total luminosity at all scales is given by the members of groups, triple systems and pairs (circles). Taking into account the contribution of non-clustered galaxies, the total luminosity density (the stepped line) gradually approaches the asymptotic value, four estimates of which according to the 2MASS survey [18–21] are marked with horizontal lines. At all scales, the local luminosity density exceeds the global value. A broad hump at the distances of 15–25 Mpc is due to the contribution of the Virgo and Fornax clusters. Since in the  $K$ -band the mean stellar mass-to-luminosity ratio of galaxies is  $M_*/L_K \simeq 1 M_\odot/L_\odot$  [19], Fig. 3 shows an excess of stellar mass density over its global value at all scales of the Local universe up to the boundary of the sample ( $D \simeq 45$  Mpc).

Summing up the virial masses of groups and clusters, Makarov and Karachentsev [9] have built the distribution of the mean density of dark matter in the spheres of various radii around our Galaxy. The results are demonstrated in Fig. 4. The contribution of groups with the population of  $n > 3$  is shown by squares, the contribution of pairs and triplets—by triangles, and the stepped line represents the course of the total mean density of matter, taking into account the non-clustered “field” galaxies, the relative contribution of which by population is 46%, and by luminosity—18%

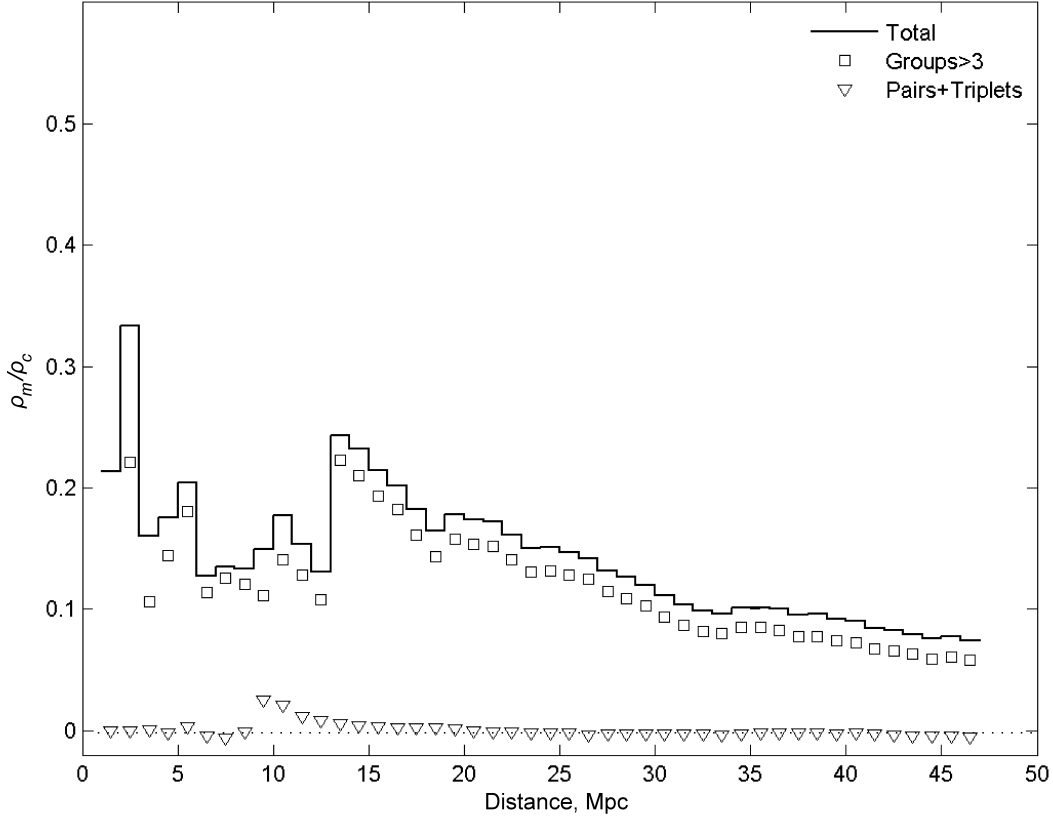


**Figure 4.** The average density of matter in the spheres of different radii (the stepped line). The squares and triangles mark the contribution of pairs, triplets, and groups of galaxies.

(the field galaxies are dominated by the dwarf population). The mass-to-luminosity ratio of the non-clustered galaxies was taken here to be the same as for pairs and triple systems, i.e. about  $20 M_{\odot}/L_{\odot}$ , which is consistent with the estimates of  $M/L_K$  from the effect of weak gravitational lensing (see [22, 23]).

As follows from the comparison of Figs. 4 and 3, the course of the mean density of dark matter with distance  $D$  approximately repeats the course of the mean stellar mass density. However, in almost all bins the density  $\Omega_m = \rho_m/\rho_c$  is below the global value  $\Omega_m = 0.28$ , and in large volumes it tends to the asymptotic value of  $\Omega_{m,loc} = 0.08 \pm 0.02$ . The error of this value is mainly determined by the measurement errors of the optical radial velocities of galaxies.

### 3. THE PROBLEM OF MISSING DARK MATTER

The observational fact that the virial masses of groups and clusters of galaxies are not able to provide the global density  $\Omega_m = 0.28$  was known in the literature for quite a while. This way, Tully [24] has used the data on 2367 galaxies with radial velocities below 3000 km/s for grouping the galaxies, applying the “hierarchical tree” technique. This technique took into account the luminosity difference of galaxies and united into groups about two thirds of all the galaxies considered. The total contribution of virial masses to  $\Omega_m$  according to Tully [24] is exactly  $\Omega_{m,\text{loc}} = 0.08$ . Vennik [25] and Magtesian [26] applied several other algorithms for clustering the galaxies in the Local universe, and obtained the following estimates:  $\Omega_{m,\text{loc}} \simeq 0.08$  and  $\Omega_{m,\text{loc}} \simeq 0.05$ , respectively. Both authors took into account the individual luminosities of galaxies.

Crook et al. [27] used the percolation method (FoF) to identify the groups of galaxies with apparent magnitudes  $K < 11.25$  from the 2MASS catalog. Fifty-three percent of all galaxies were clustered at the average density contrast of  $\Delta\rho/\rho \sim 80$ . Their total contribution in  $\Omega_m$  amounted to 0.10–0.13 depending on the method of virial mass estimation. The differences in luminosity of galaxies were ignored here. Trying to “reach out” to the global value of  $\Omega_m = 0.28$ , Crook et al. [27] made another version of the group catalog with a softer condition for the average density contrast  $\Delta\rho/\rho \sim 12$ . This technique fitted 73% of galaxies into groups and clusters, and the contribution of galaxy systems in  $\Omega_m$  amounted to 0.14–0.23. However, most of these low-contrast aggregates are not virialized systems, since their crossing time is comparable with the age of the Universe or even exceeds it.

Bahcall et al. [28] considered the contribution to  $\Omega_m$  of systems of galaxies at all scales—from pairs to superclusters. Assuming that the main contribution to  $\Omega_m$  is introduced by rich clusters, the authors obtained the value of  $\Omega_m = 0.16 \pm 0.05$ . However, despite an increase in the average virial mass-to-luminosity ratio from pairs and groups to clusters and superclusters, the main contribution to  $\Omega_m$  is still made by the small systems like the Local Group. Only 2% of the  $K$ -band luminosity falls on the clusters richer than Virgo [29], and the relative fraction of virial mass in them does not exceed 10–15%. Note that in the volume we consider ( $V_{\text{LG}} < 3500$  km/s) the relative contribution of the Virgo cluster in the total mass of the Local universe is about 15%, i.e. it is not determinative on the background of less populated systems.

Thus, the most refined methods of estimating the virial mass in systems of different size and population lead to the value of the local ( $D \leq 50$  Mpc) average density of matter of  $\Omega_{m,\text{loc}} = 0.08 \pm 0.02$ , what is 3–4 times lower than the global value of  $\Omega_{m,\text{glob}} = 0.28 \pm 0.03$  in the standard  $\Lambda$ CDM cos-



mology [30, 31]. Various possible explanations of this contradiction were proposed in the literature. We shall list three of them here.

1) Dark matter in the systems of galaxies extends far beyond their virial radius, so that the total mass of a group/cluster is 3–4 times larger than the virial estimate.

2) The diameter of the considered region of the Local universe, 90 Mpc, does not correspond to the true scale of the “homogeneity cell”; our Galaxy may be located inside a giant void sized about 100–500 Mpc, where the mean density of matter is 3 to 4 times lower than the global value.

3) Most of the dark matter in the Universe, or about two thirds of it is not associated with groups and clusters of galaxies, but distributed in the space between them in the form of massive dark clumps or as a smooth “ocean.”

Let us discuss each of these hypotheses in more detail.

### 3.1. Dark Halos around Groups and Clusters

Tavio et al. [32] and Masaki et al. [33] considered the integral distribution of dark halo mass as a function of distance, expressed in the units of virial radius. Assuming a standard NFW-profile of the halo, they estimated that about 50% of the total mass is located outside the virial radius. According to Rines and Diaferio [34], the collapse region surrounding a galaxy cluster between the radii of  $R_{\text{VIR}}$  and  $R_0 \simeq 3.7R_{\text{VIR}}$  may be containing a mass of  $(1.19 \pm 0.18)M_{\text{VIR}}$ .

On the other hand, the modelling of orbits of test particles inside a massive halo, performed in [35] made these authors conclude that the ratio of the total halo mass to the virial mass is on the average only  $M_T/M_{\text{VIR}} = 1.25$ . We consider this result to be more realistic. As we noted in the introduction, the total mass estimates of the Local Group and other nearby groups within a radius of  $R_0$  are in good agreement with their virial masses. A similar correspondence (with an error of 30–50%) was also found in the closest to us Virgo and Fornax clusters [36, 37]. In any case, the assumption of the presence between  $R_{\text{VIR}}$  and  $R_0$  of a mass 2 to 3 times larger than  $M_{\text{VIR}}$  clearly contradicts the existing observational data.

### 3.2. Extended Local Void

The idea that our Galaxy is located near the center of a vast cosmic void [38, 39] was repeatedly set forth as an alternative to the model of accelerated expansion of the Universe, created based on observations of distant Supernovae. However, as indicated by the data in Figs. 3 and 4, the

location of our Galaxy is characterized by an excess, rather than by a deficiency of local density at all scales up to 45 Mpc. It can be assumed that the local density excess elevates above the extended surrounding void like the central peak of a lunar crater. Apart from its slight artificiality, this assumption is in contradiction with observational data. The counts of galaxies in the  $K$ -band, made up to the deep limit in different directions [40–43] do not show any signs of the existence of an extensive local void sized about 100–500 Mpc.

### 3.3. *The Population of Dark Attractors*

For obvious reasons, the hypothesis of the existence between galaxy groups and clusters of a large number of invisible dark halos with different masses is difficult to prove observationally. Nevertheless, there already exist some evidence in favor of such an unusual picture. Karachentsev et al. [44] drew attention to the presence among the isolated galaxies listed in the KIG catalog [45] of a fraction of objects with heavily distorted structures. A good example is the KIG 293 = UGC 4722 galaxy with an extended curved tail (Fig. 5). It is commonly assumed that the structures like these are formed during a tight interaction of galaxies of an approximately equal mass. However, in the broad vicinity of UGC 4722 there are no neighbors that would be able to produce the observed tidal perturbations. As a probable explanation for this phenomenon we may assume here a case of interaction of a normal galaxy with an invisible dark object having a mass of about  $10^9 M_\odot$ . Recently, a similar population of distorted isolated galaxies was found in the Local Orphan Galaxy catalog [17]. In both samples, KIG and LOG, the relative number of such objects is small, about 4%.

Examining the structures of the Einstein gravitational lenses with the Hubble Space Telescope, Vegetti et al. [46, 47] have discovered at the cosmological distances of  $z = 0.22$  and  $z = 0.88$  two cases, indicating the presence of invisible companions around the lens galaxies. According to the authors, the masses of these dark companions amount to  $10^8$ – $10^9 M_\odot$ , and the lower limit of their mass-to-luminosity ratio exceeds  $120 M_\odot/L_\odot$ . It is as yet viewed difficult to evaluate the cosmic abundance of such dark substructures.

Shan et al. [48] investigated the effects of weak gravitational lensing of distant galaxies in an area sized  $72^\circ$ , recorded at the CFHT telescope with subarcsecond images. On the map of gravitational potential peaks, reconstructed from these data, the authors have found 301 peaks, 126 of which were identified with the optical or X-ray clusters of galaxies. About 60% of the peaks remained unidentified, which may indicate the existence at the epoch of  $z \sim 0.4$  of the population of dark attractors with masses, typical of rich clusters of galaxies. Similar observational arguments in favor

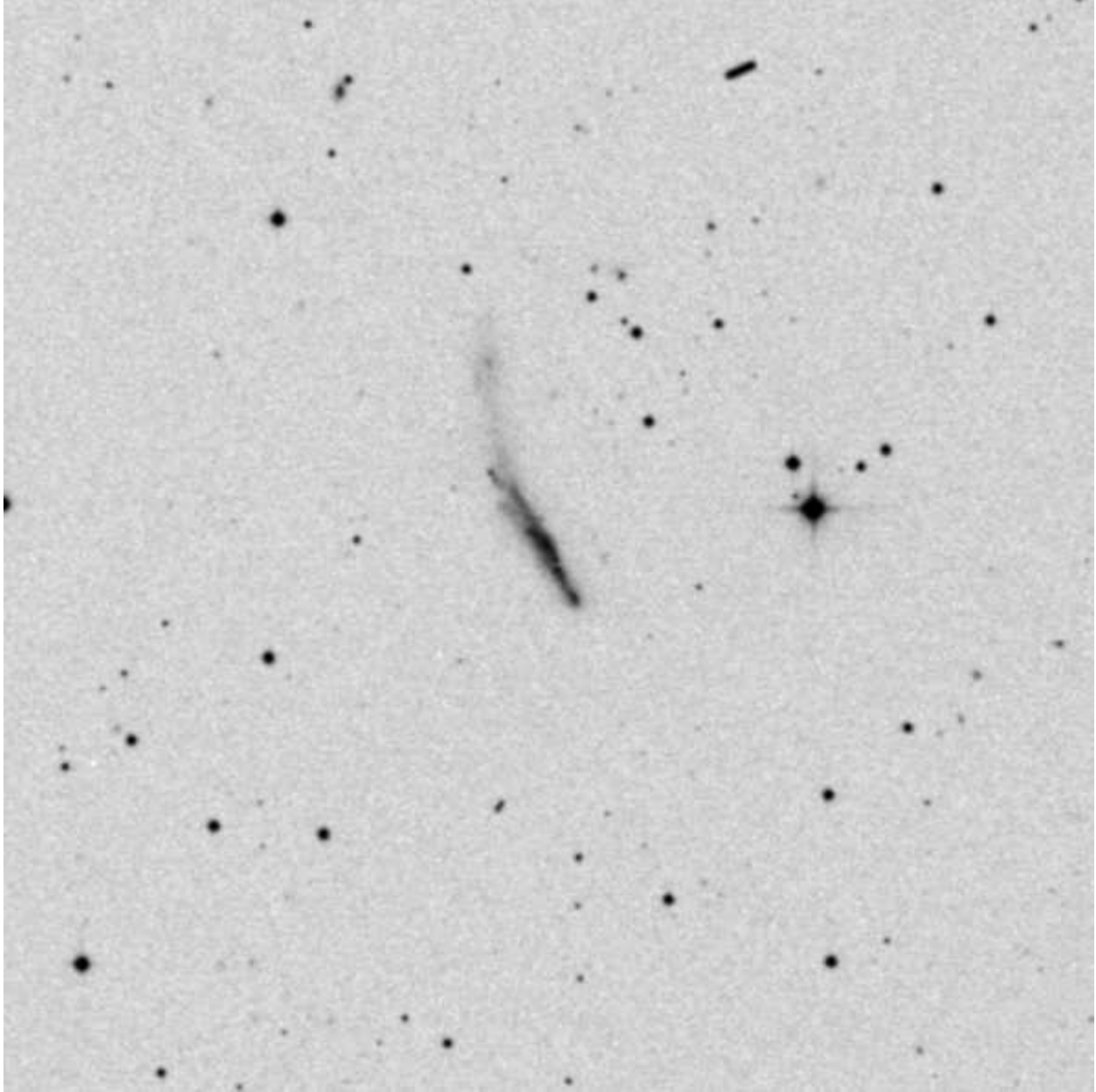


**Figure 5.** An isolated galaxy UGC 4722 with signs of a strongly perturbed structure. The image size is  $10' \times 10'$ . The short bold strip in the upper right is a trace of an asteroid.

of the existence of massive dark clumps were given earlier by Natarajan and Springel [49] and Jee et al. [50] based on the effects of weak lensing.

Among the galaxies of the Local universe with measured distances and radial velocities there exist galaxies with large negative peculiar velocities. Inspecting these cases, Karachentsev et al. [51] noted the fact that a half of these rapidly moving galaxies are concentrated in a small region of the sky ( $RA \simeq 12^h 20^m, Dec \simeq +30^\circ$ ), called the Coma I

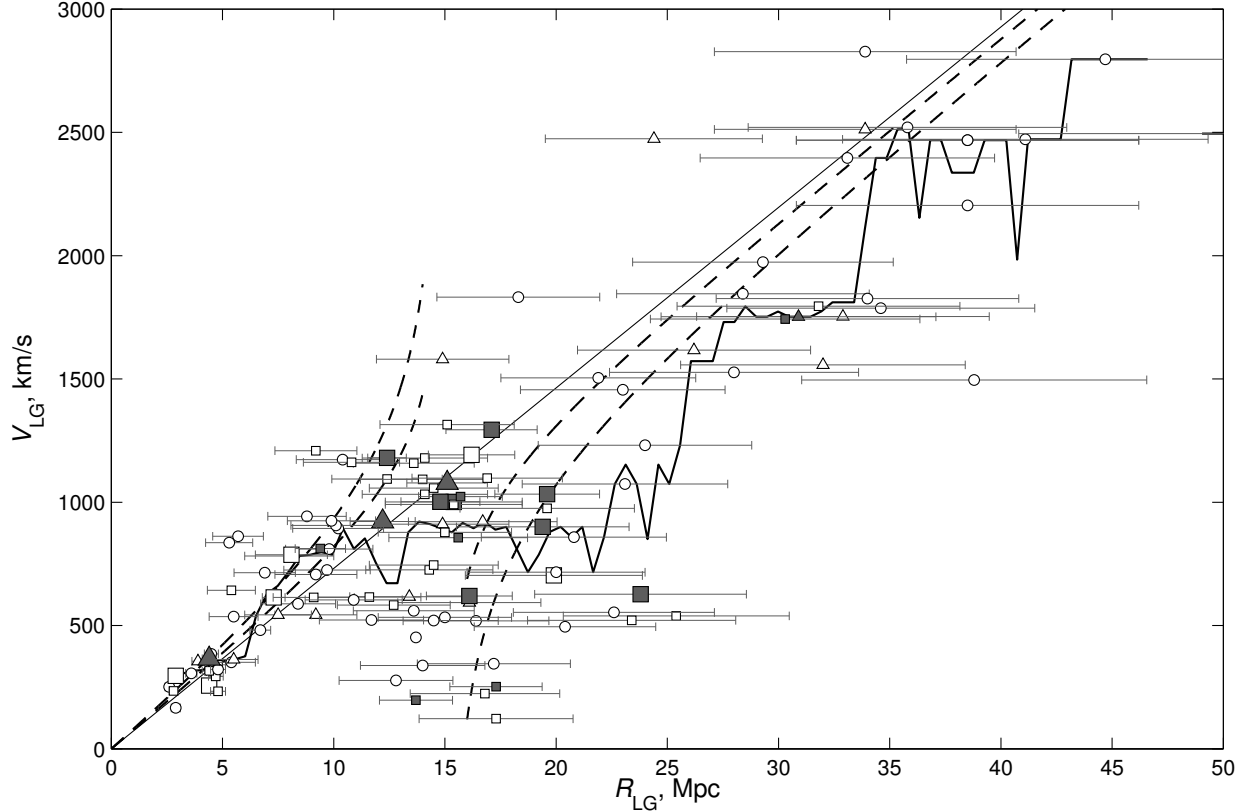


**Figure 6.** The velocity–distance relation for 122 galaxies in the Coma I region. The straight line corresponds to the unperturbed Hubble flow with the parameter  $H_0 = 73$  km/s/Mpc. The squares mark the group members, the triangles denote the members of triplets and pairs, and the circles—single galaxies. The galaxies with bulges (E, S0, Sa) are shown by dark symbols. The horizontal segments correspond to the distance measurement errors. The broken line describes the behavior of the running median with a window of 2 Mpc. Two dashed lines correspond to the pattern of galaxy infall on a point-like attractor with a mass of  $0.5 \times 10^{14} M_\odot$  and  $2.0 \times 10^{14} M_\odot$ , located at a distance of 15 Mpc, for the case where the line of sight passes through the center of the attractor.

cloud. This region contains some scattered groups with the distances of 4 to 30 Mpc. The Hubble diagram for the Coma I galaxies (Fig. 6) reveals systematic deviations from the linear relation  $V = H_0 R$ , characteristic of the infall of galaxies into the attractor. The effect of infall is consistent with the observational data at the attractor mass amounting to around  $2 \times 10^{14} M_\odot$  at a distance of about 15 Mpc from us. The total luminosity of galaxies in the zone of the assumed attractor is  $L_K = 1.0 \times 10^{12} L_\odot$ , which gives the mass-to-luminosity ratio of  $M/L_K \sim 200 M_\odot/L_\odot$ . This  $M/L_K$  ratio is 4 times higher than that found in rich clusters like Coma. It is possible that we have come across the first case of a nearby dark attractor having a mass, typical of clusters of galaxies.

It should be emphasized that the mean local matter density  $\Omega_m$  can be determined not only by

summing the virial masses of galaxy systems, but also from the analysis of the peculiar velocity field at sufficiently large scales. Abate and Erdogdu [52] investigated the peculiar velocity field of galaxies from the SFI++ sample [53] and at the scale of about 6000 km/s obtained the estimate of  $\Omega_m = 0.09\text{--}0.23$ . This value should obviously include the dark matter between the groups and clusters, if it exists.

A similar analysis of the SFI++ sample was made by Davis et al. [54] involving the data on redshifts of galaxies from the 2MASS survey [55]. The authors deduced that the local field of peculiar velocities is in a good agreement with the local topography of gravitational potential (the distribution of dark matter follows the distribution of galaxies). However, Davis et al. specify that the smooth component of dark matter can not be tested by the means of this technique. Another local estimate  $\Omega_m = 0.20 \pm 0.07$  at the scale of approximately 100 Mpc is obtained in [56] based on the behavior of the clustering dipole of 2MASS galaxies relative to the direction of motion of the Local Group in the cosmic microwave background radiation frame.

#### 4. DYNAMIC COMPONENTS OF THE LARGE-SCALE STRUCTURE

The following elements of the large-scale structure of the Universe are typically singled out based on their geometric features: large and small cosmic voids, filaments and walls bordering the voids, clusters of galaxies in the nodes at intersections of the filaments and walls. As the Universe expands, the density perturbations increase and the elements of the large-scale structure become more contrasting, which is clearly illustrated by numerous N-body simulations.

From the dynamic point of view, it is reasonable to divide the elements of the large-scale structure into three categories:

- a) virialized zones of groups and clusters, where the balance between the kinetic and potential energy ( $2T + U = 0$ ) was established, and the galaxies have “forgotten” the initial conditions of their formation;
- b) collapsing regions around the virialized zones, limited by the zero velocity spheres with the  $R_0$  radius;
- c) the remaining, infinitely expanding regions of the “general field” which comprise the population of voids and diffuse filaments.

An example of such a separation is shown in Fig. 7, which represents a complex of nearby groups in the Fornax-Eridanus constellations in equatorial coordinates [37]. Here the virialized regions of the Fornax cluster (located downward from the center of the figure) and the groups, adjacent to

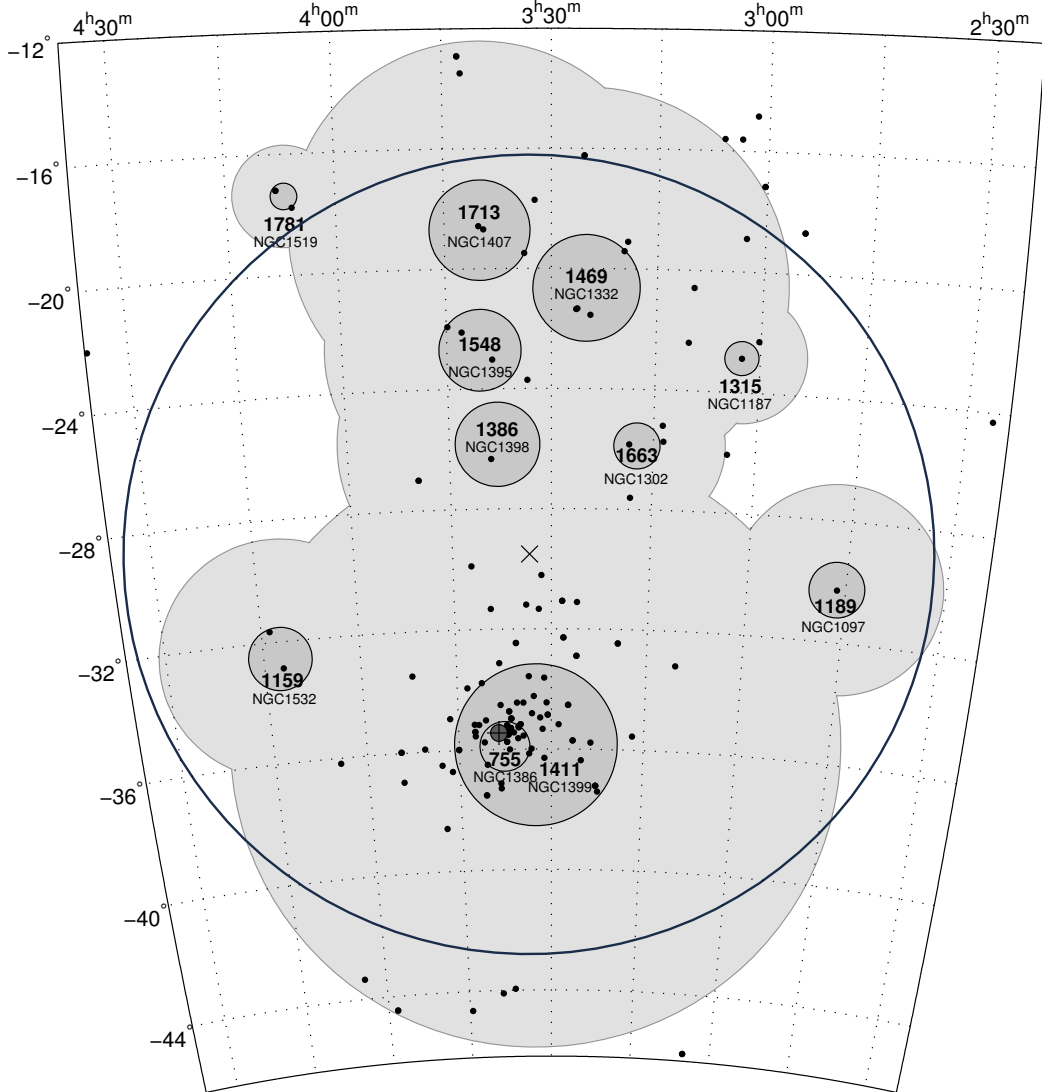


**Figure 7.** The Fornax cluster and Eridanus groups of galaxies in equatorial coordinates. The dark circles correspond to the virial radii of the systems, the lighter circles correspond to the zones of collapse around them. The NGC numbers mark the brightest members of each group, and the figures in bold—the mean radial velocities of groups in km/s.

each other in the Eridanus are marked by dark circles. The lighter circles correspond to the  $R_0$  radii around the groups. It is clear from the figure that the spheres of  $R_0$  radius mutually intersect, forming a surface, under which the Eridanus groups and the Fornax cluster will merge into a single dynamic aggregate over time.

Based on the results of clustering of galaxies in the Local universe [9] and other observational data on similar systems, it is possible to identify a number of important parameters, characterizing the dynamic status of three components of the large-scale structure at the current epoch. These parameters are listed in the table. Some of them as yet contain a significant uncertainty.

**Table 1.** Basic parameters of three dynamic regions in the large-scale structure

Basic parameters	Virialized	Collapsing	Remaining
	zones	regions	expanding background
Relative number of galaxies	54%	$\sim 20\%$	$\sim 26\%$
Relative amount of stellar mass	82%	$\sim 8\%$	$\sim 10\%$
Relative fraction of occupied volume	0.1%	5%	95%
Contribution to $\Omega_m$	0.06	0.02	0.20
Mean ratio of dark to stellar mass, $M_{\text{DM}}/M_*$	$\sim 26$	$\sim 87$	$\sim 690$

As follows from the first two rows in the table, more than a half of all galaxies and more than four fifths of their stellar mass are already located within the virial zones. The subsequent infall of galaxies from the surrounding collapsing regions will bring a relatively small addition to the existing virial masses. In this sense we can say that the main stage of dynamical evolution of the large-scale structure is already completed.

The third row of the table shows that the virialized volumes of groups and clusters occupy only 0.1% of the total volume, while the collapse regions around them take up about 5% of the volume of Universe. The remaining 95% of the volume, related to the general field contain only about 10% of stellar mass. Thus, the contrast of the mean stellar mass density between the virialized volumes and the general field reaches about 7000.

The penultimate row of the table demonstrates the contribution of three different dynamic zones to  $\Omega_m$ , considering that overall they yield a default value of  $\Omega_{m,\text{glob}} = 0.28$ . It is interesting to note here that the contrast of the average densities of dark matter between the virialized zones and the general field is about 280.

Finally, the last line presents the characteristic ratio of the dark matter mass to the luminous (stellar) mass in the three designated regions. As above, the stellar mass of the galaxy  $M_*$  is expressed in terms of its  $K$ -band luminosity, assuming that  $M_*/L_K \simeq 1.0 M_\odot/L_\odot$  [19].

One important circumstance should be noted here. The algorithm, applied in [9] for the selection of groups assumes that in all galaxies, irrespective of their luminosity, type or surrounding density, the ratio of the total mass of the halo to the mass of the stellar component has one and the same value,  $M_T/M_* = 6$ . This dimensionless quantity is the only more or less arbitrary parameter of the applied algorithm (as opposed to the percolation algorithm FoF, where the choice of two arbitrary parameters is required: the maximal difference in radial velocities and the maximal projected separation of the components of a virtual pair). According to the ‘‘Bolshoi’’ N-body simulations within the  $\Lambda$ CDM model [57], the  $M_T/M_* = 6$  ratio should approximately be met (within the  $\pm 1\sigma$  band)

for all the galaxies with stellar masses in the range of  $\log(M_*/M_\odot) = [8.5-11.0]$ , which indirectly justifies the choice of the single clustering parameter  $M_T/M_*$ .

Thus, using the initial value of  $M_T/M_* = 6$  for individual halos of galaxies, for the virialized regions of groups and clusters we get the mean ratio of  $M_T/M_* \simeq 26$  (it systematically grows in the transition from pairs and groups to clusters), and the remaining space of the general field is characterized by the ratio  $M_T/M_* \sim 690$ , i.e. two orders higher than that of a typical galaxy.

## 5. CONCLUDING REMARKS

As it is widely known, some predictions of the standard  $\Lambda$ CDM cosmological model are not well consistent with the observational data available nowadays. First and foremost, this concerns the problem of “missing satellites” [58], which lies in the fact that the theory predicts the number of companions in the Milky Way-type galaxies to be dozens of times greater than that observed around our Galaxy, M 31, and other neighboring high-luminosity galaxies. Various explanations of this inconsistency have been proposed, based on some features of the star formation process in dwarf galaxies at the  $z \sim 10$  epoch. However, the problem of “missing satellites” still remains.

Another puzzle is that the theory of formation of chemical elements in the hot expanding Universe gives the value of cosmic baryon abundance of  $\Omega_b = 0.045 \pm 0.005$  [30]. However, the current observational data reveal only 1/10 of these baryons, existing in the form of stars and gas in the galaxies. It is assumed that the bulk of the baryons may be distributed between the galaxies alike the warm ( $T \sim 10^5$  K), non-virialized “broth” [59]. There have been reports in the literature on the likely observational detection of “missing baryons” [60, 61]. Nevertheless, this problem can neither be considered definitively resolved.

A significant divergence between the local ( $0.08 \pm 0.02$ ) and global ( $0.28 \pm 0.03$ ) values of the average matter density adds yet another mystery, the problem of “missing dark matter”. Unlike the situation with missing companions and baryons, the lack of dark matter in the Local universe is not characterized by one or two orders of magnitude, but only by a factor of 3, which, however, is quite a few for the so-called “precision cosmology era”. Contradictory estimates of  $\Omega_m$  probably indicate that the assumption of proportional distribution of dark and stellar matter,  $\log(\rho_{\text{DM}}) \propto \log(\rho_*)$ , though being convenient, is however not quite a justifiable paradigm. In other words, our Universe might happen to be more hidden and dark than we thought until recently.



## ACKNOWLEDGMENTS

I thank James Peebles for valuable comments. This work was supported by the grant of the Russian Foundation for Basic Research (grant no. 11-02-90449-Ukr-f-a) and by the state contract “Cosmology of Nearby Universe” no. 14.740.11.0901.

- 
1. P. J. E. Peebles, *Principles of Physical Cosmology* (Princeton University Press, 1993).
  2. P. J. E. Peebles, S. D. Phelps, E. J. Shaya and R. B. Tully, *Astrophys. J.* **554**, 104 (2001).
  3. P. J. E. Peebles and A. Nusser, *Nature* **465**, 565 (2010).
  4. M. G. Lee, W. L. Freedman and B. F. Madore, *Astronom. J.* **106**, 964 (1993).
  5. I. D. Karachentsev, V. E. Karachentseva, W. K. Huchtmeier and D. I. Makarov, *Astronom. J.* **127**, 2031 (2004).
  6. I. D. Karachentsev, O. G. Kashibadze, D. I. Makarov and R. B. Tully, *Monthly Notices Roy. Astronom. Soc.* **393**, 1265 (2009).
  7. I. D. Karachentsev, *Astronom. J.* **129**, 178 (2005).
  8. I. D. Karachentsev, D. I. Makarov and E. I. Kaisina, in preparation (RCNG) (2012).
  9. D. I. Makarov and I. D. Karachentsev, *Monthly Notices Roy. Astronom. Soc.* **412**, 2498 (2011).
  10. K. N. Abazajian, J. K. Adelman-McCarthy, M. A. Agueros et al., *Astrophys. J. Suppl.* **182**, 543 (2009).
  11. P. Papai and I. Szapudi, *Astrophys. J.* **725**, 2078 (2010).
  12. M. J. Meyer, M. A. Zwaan, R. L. Webster et al., *Monthly Notices Roy. Astronom. Soc.* **350**, 1195 (2004).
  13. R. Giovanelli, M. P. Haynes, B. R. Kent et al., *Astronom. J.* **130**, 2598 (2005).
  14. J. P. Huchra and M. J. Geller, *Astrophys. J.* **257**, 423 (1982).
  15. I. D. Karachentsev and D. I. Makarov, *Astrophysical Bulletin* **63**, 299 (2008).
  16. D. I. Makarov and I. D. Karachentsev, *Astrophysical Bulletin* **64**, 24 (2009).
  17. I. D. Karachentsev, D. I. Makarov, V. E. Karachentseva and O. V. Melnyk, *Astrophysical Bulletin* **66**, 1 (2011).
  18. S. Cole, P. Norberg, C. M. Baugh et al., *Monthly Notices Roy. Astronom. Soc.* **326**, 255 (2001).
  19. E. F. Bell, D. H. McIntosh, N. Katz and M. D. Weinberg, *Astrophys. J. Suppl.* **149**, 289 (2003).
  20. C. S. Kochanek, M. A. Pahre, E. E. Falco et al., *Astrophys. J.* **560**, 566 (2001).
  21. D. H. Jones, B. A. Peterson, M. Colless and W. Daunders, *Monthly Notices Roy. Astronom. Soc.* **369**, 25 (2006).
  22. R. Mandelbaum, U. Seljak, G. Kauffmann et al., *Monthly Notices Roy. Astronom. Soc.* **368**, 715 (2006).
  23. E. van Uitert, H. Hoekstra, M. Velander et al., *Astronom. and Astrophys.* **534**, 14 (2011).
  24. R. B. Tully, *Astrophys. J.* **321**, 280 (1987).

25. J. Vennik, *Tartu Astron. Obs. Publ.* **73**, 1 (1984).
26. A. Magtesian, *Astrofizika* **28**, 150 (1988).
27. A. C. Crook, J. P. Huchra, N. Martimbeau et al., *Astrophys. J.* **655**, 790 (2007).
28. N. A. Bahcall, R. Cen, R. Dave et al., *Astrophys. J.* **541**, 1 (2000).
29. V. R. Eke, C. M. Baugh, S. Cole et al., *Monthly Notices Roy. Astronom. Soc.* **362**, 1233 (2005).
30. M. Fukugita and P. J. E. Peebles, *Astrophys. J.* **616**, 643 (2004).
31. D. N. Spergel et al., *Astrophys. J. Suppl.* **170**, 377 (2007).
32. H. Tavo, A. J. Cuesta, F. Prada et al., arXiv:0807.3027 (2008).
33. S. Masaki, M. Fukugita and N. Yoshida, arXiv:1105.3005 (2011).
34. K. Rines and A. Diaferio, *Astronom. J.* **132**, 1275 (2006).
35. D. Anderhalden and J. Diemand, *Monthly Notices Roy. Astronom. Soc.* **414**, 3166 (2011).
36. I. D. Karachentsev and O. G. Nasonova, *Monthly Notices Roy. Astronom. Soc.* **405**, 1075 (2010).
37. O. G. Nasonova, J. A. de Freitas Pacheco and I. D. Karachentsev, *Astronom. and Astrophys.* **532**, 104 (2011).
38. A. Shafieloo, V. Sahni and A. A. Starobinsky, arXiv:0903.5141 (2009).
39. A. E. Romano, M. Sasaki and A. A. Starobinsky, arXiv:1006.4735 (2010).
40. S. Djorgovski, B. T. Soifer, M. A. Pahre et al., *Astrophys. J.* **438**, L13 (1995).
41. M. A. Bershad, J. D. Lowenthal and D. C. Koo, *Astrophys. J.* **505**, 50 (1998).
42. T. Totani, Y. Yoshii, T. Maihara et al. *Astrophys. J.* **559**, 592 (2001).
43. J. S. Huang, D. Thompson, M. W. Kummel et al., *Astronom. and Astrophys.* **368**, 787 (2001).
44. I. D. Karachentsev, V. E. Karachentseva and W. K. Huchtmeier, *Astronom. and Astrophys.* **451**, 817 (2006).
45. V. E. Karachentseva, *Soobscheniya SAO* **8**, 3 (1973).
46. S. Vegetti, L. Koopmans, A. Bolton et al, *Monthly Notices Roy. Astronom. Soc.* **408**, 1969 (2010).
47. S. Vegetti, D. J. Lagattuta, J. P. McKean et al, arXiv:1201.3643 (2012).
48. H. Y. Shan, J. P. Kneib, C. Tao et al., arXiv:1108.1981 (2011).
49. P. Natarajan and V. Springel, *Astrophys. J.* **617**, L13 (2004).
50. M. J. Jee, R. L. While, N. Benitez et al., *Astrophys. J. Suppl.* **618**, 46 (2005).
51. I. D. Karachentsev, O. G. Nasonova and H. M. Courtois, *Astrophys. J.* **743**, 123 (2011).
52. A. Abate and P. Erdogdu, *Monthly Notices Roy. Astronom. Soc.* **400**, 1541 (2009).
53. C. M. Springov, K. L. Masters, M. P. Haynes et al., *Astrophys. J. Suppl.* **172**, 599 (2009).
54. M. Davis, A. Nusser, K. Masters et al., *Monthly Notices Roy. Astronom. Soc.* **413**, 2906 (2011).
55. T. N. Jarrett, T. Chester, R. Cutri et al., *Astronom. J.* **119**, 2498 (2000).
56. M. Bilicki, M. Chodorowski, G. A. Mamon and T. Jarrett, *Astrophys. J.* **741**, 31 (2011).
57. S. Trujillo-Gomez, A. A. Klypin, J. Primack and A. J. Romanowsky, *Astrophys. J.* **742**, 16 (2011).
58. A. Klypin, A. V. Kravtsov, O. Valenzuela and F. Prada, *Astrophys. J.* **522**, 82 (1999).
59. R. Cen and J. P. Ostriker, *Astrophys. J.* **519L**, 109 (1999).

60. J. T. Stocke, S. V. Penton, C. W. Danforth et al., *Astrophys. J.* **641**, 217 (2006).
61. A. Naranayan, B. P. Wakker, B. D. Savage et al., *Astrophys. J.* **721**, 960 (2010).